Clin Exp Immunol 1996; **103**:316–321

Tissue-dependent differences in the asynchronous appearance of mast cells in normal mice and in congenic mast cell-deficient mice after infusion of normal bone marrow cells

T. DU*†, D. S. FRIEND*†‡, K. F. AUSTEN*† & H. R. KATZ*† *Department of Medicine, Harvard Medical School, †Division of Rheumatology and Immunology, and ‡Department of Pathology, Brigham and Women's Hospital, Boston, MA, USA

(Accepted for publication 28 September 1995)

SUMMARY

The time courses of the appearance of tissue mast cells in six sites were compared in normal WBB6F$_1$-+/+ mice (+/+) and in congenic mast cell-deficient WBB6F$_1$-W/W^v mice (W/W^v) that received an intravenous infusion of bone marrow cells from +/+mice (BM $\rightarrow W/W^v$). As assessed by morphometric analysis of Carnoy's solution-fixed, methylene blue-stained tissue sections, the density of mast cells in the stomach mucosa, stomach submucosa, and spleen of +/+ mice reached maximal levels by 8 weeks of age, whereas the density of mast cells in the skin, extraparenchymal airway walls, and lung parenchyma did not reach maximal levels until 18 weeks of age. When 8-week-old W/W^v mice were infused with 2×10^7 bone marrow cells from +/+ mice, mast cells appeared in the stomach mucosa and submucosa after 2·5 weeks, in the spleen and extraparenchymal airway walls after 5 weeks, and in the lung parenchyma after 10 weeks. Twenty weeks after bone marrow infusion, the mast cell densities in the spleen, stomach mucosa, and stomach submucosa were seven-, 13-, and five-fold greater, respectively, than those in age-matched +/+ mice, but were eight-, two-, and five-fold lower in the skin, extraparenchymal airway walls, and lung parenchyma, respectively. Thus, those tissues that in +/+ mice reached maximal mast cell densities earlier exhibited abnormally high mast cell densities in BM $\rightarrow W/W^v$ mice, and those that reached maximal mast cell densities later in +/+ mice had abnormally low mast cell densities in BM $\rightarrow W/W^v$ mice. Immunological and inflammatory responses are often compared in W/W^v and BM$\rightarrow W/W^v$ mice to assess mast cell dependency. Our results indicate that the capacity to restore a mast cell-dependent response in a particular tissue of the latter mice may relate to the local mast cell density and whether the immunological challenge activates mast cells only in that tissue or systematically with attendant widespread release of proinflammatory mediators.

Keywords mast cells ontogeny morphometrics

INTRODUCTION

Mast cells, through their activation-induced release of a large number of proinflammatory mediators, are key effector cells of allergic inflammation. Two types of mast cells were initially described in rodents, based on the ability of their secretory granules to bind cationic dyes after tissue sections were exposed to different fixatives. Either Carnoy's solution (ethanol/chloroform/acetic acid, 6 : 3 : 1, v/v), or fixatives containing no more than 0·4–0·8% formaldehyde are required for staining of mucosal mast cell granules with methylene blue, toluidine blue, or alcian blue [1–3]. In contrast, the granules of connective tissue mast cells in the skin and other organs can be stained after fixation with these fixatives as well as with 10% neutral buffered formalin.

Correspondence: Dr Howard R. Katz, Seeley G. Mudd Building, 250 Longwood Avenue, Boston, MA02115, USA.

W/W^v mutant mice are mast cell-deficient, with less than 1% the density of mast cells of +/+ mice in skin, and no detectable mast cells in other organs [4]. The mast cell deficiency results from a mutation that inhibits the tyrosine kinase activity of the c-*kit* receptor for the c-*kit* ligand [5]. The injection of bone marrow cells from congenic +/+ mice into W/W^v mice elicits the appearance of tissue mast cells [4], which in the stomach mucosa and peritoneal cavity are phenotypically indistinguishable from mast cells in the corresponding sites of +/+ mice [6,7].

We now report on the time-related appearance of mast cells in multiple issues of +/+ and BM $\rightarrow W/W^v$ mice. The results indicate that the age-dependent appearance of mast cells in

different tissues of $+/+$ mice proceeds with two distinct kinetic patterns. Furthermore, the density of both mucosal and connective tissue-type mast cells in BM $\rightarrow W/W^v$ mice may be abnormally high or low at different tissue sites, relative to the mast cell populations at those sites in age-matched $+/+$ mice. The studies suggest that the entry in mast cell progenitors into tissues differs both among organs and in individual organs with ageing of the animal. In addition, the studies indicate that when BM $\rightarrow W/W^v$ mice are used to define a role for mast cells in an inflammatory response, with $+/+$ mice serving as the frame of reference, the potential influence of the abnormal mast cell densities on the outcome should be considered.

MATERIALS AND METHODS

Animals and bone marrow cell transplantation

Male W/W^v and $+/+$ mice were obtained from The Jackson Laboratory (Bar Harbor, ME). Eight-week-old W/W^v mice were injected intravenously through the tail vein with 2×10^7 fresh $+/+$ bone marrow cells that contain agranular mast cell progenitors [4,8]. Mice were infused in two groups and studied at 1 and 2·5 weeks or 5, 10, 15, and 20 weeks after bone marrow infusion, respectively. Age-matched, uninjected W/W^v and $+/+$ mice served as controls.

Tissue preparation

At 1, 2·5, 5, 10, 15 and 20 weeks after bone marrow infusion, six BM $\rightarrow W/W^v$ mice were anaesthetized by the injection of 10% barbital sodium intraperitoneally and were killed by opening the abdominal cavity and cutting the aorta, the inferior vena cava, and the portal vein. Uninjected W/W^v and $+/+$ mice, six in each group, were killed at 8, 18 and 28 weeks of age.

The lungs with trachea attached were removed from each mouse and fixed by intrabronchial perfusion with Carnoy's solution at a constant pressure of 25 cm H_2O at room temperature for 3 h. Portions of ear (as a source of skin), spleen, stomach, and liver from the same animals were fixed in Carnoy's solution for 8 h. After fixation, the tissues were immersed in 100% methanol at -20°C for 12 h.

Tissues were embedded in paraffin, and 4-μm sections were cut on a Reichert-Jung Model 2065 supercut rotary microtome (Leica, Deerfield, IL). The lungs were cut from the hilar side sagitally, and sections of other tissues were cut cross-sectionally. The sections were stained for 10 min in a 5% (w/v) ethanolic solution of methylene blue.

Morphological and morphometric studies

Sections were observed by oil immersion brightfield microscopy, and the numbers of mast cells in an area of interest were counted. Except for the lung, the technique for morphometric measurement has been described previously [9,10]. Briefly, outlines of ear skin, spleen, stomach, liver, and extraparenchymal airway walls, including the trachea and main bronchi, were traced on paper with a Nikon drawing tube attachment and then measured with a computer-controlled digitizing board and commercial software (Jandel Scientific, Corte Madera, CA).

Areas of lung parenchyma and air space were determined with a computer image analysis program. Briefly, the microscopic images were captured by a video camera (Newvicon, Panasonic PV 1450), digitized by a real time frame grabber (Coreco Oculus 200), and stored in a microcomputer. Lung parenchyma and airspace were identified by their characteristic colours. The proportion of the image occupied by lung parenchyma or airspace was quantified by counting the number of picture elements with the corresponding colour [9].

Data analyses

The areas of ear skin were determined by subtracting the cross-sectional area of the cartilage from the cross-sectional ear area. Extraparenchymae airway walls were evaluated for the airway lumen, defined as the area circumscribed by the basement membrane of epithelium (LuB) and the outer border of the airway wall (Ae). The area of the airway wall (Aw) was calculated as the difference between Ae and LuB [11]. Airways whose ratio of maximal to minimal internal diameter were $\geqslant 2$ were considered to be cut obliquely and were not measured.

For stomach, only the glandular region was studied, and the stomach wall was separated into two compartments. The area between the epithelial surface and the internal border of the muscularis mucosa was designated as 'mucosa'. The area that included the smooth muscle layers and serosa was designated as 'submucosa'.

The densities of mast cells in tissues were calculated per mm^2 and are expressed throughout as mean $\pm$ s.e.m. Comparisons of the mean mast cell densities between animal groups were made with a *t*-test for unpaired data. $P < 0{\cdot}05$ was defined as significant.

RESULTS

Morphometric analysis of mast cell densities in the tissues of $+/+$ and BM $\rightarrow W/W^v$ mice: skin

A small number of native mast cells were detected in the ear skin of 8-week-old W/W^v mice ($1{\cdot}155 \pm 0.945$ cells/mm^2), and only one of six 28-week-old W/W^v mice had skin mast cells (Fig. 1). Mast cell densities in the skin of 8-, 18-, and 28-week-old $+/+$ mice were significantly greater than those of age-matched W/W^v mice ($P < 0{\cdot}002$). After the intravenous infusion of bone marrow cells from $+/+$ mice, the density of the skin mast cells increased progressively in the recipients from 10 weeks after infusion, but the increase did not achieve statistical significance until 20 weeks after infusion. At that time, the density of mast cells in the skin was significantly greater than the density in W/W^v mice and in BM $\rightarrow W/W^v$ mice at 1, 2·5, 5 and 10 weeks after infusion ($P < 0{\cdot}04$). However, the density of skin mast cells in BM $\rightarrow W/W^v$ mice at 20 weeks was still five- to eight-fold lower than the density in skin of $+/+$ mice at any age examined ($P < 0{\cdot}0001$).

Extraparenchymal airway walls

No mast cells were detected in the walls of extraparenchymal airways, including the trachea and main bronchi, of W/W^v mice at any time point examined (Fig. 2a). In $+/+$ mice, mast cell densities in airway walls increased significantly from 8-week-old to 18- and 28-week-old animals ($P < 0{\cdot}05$). Mast cells appeared in the extraparenchymal airway walls of BM $\rightarrow W/W^v$ mice at 5 weeks after bone marrow infusion. The density of airway wall mast cells increased progressively, and peaked at 15 weeks after bone marrow infusion at a significantly greater level than that at 5 weeks after infusion ($P < 0{\cdot}005$), but not significantly greater than at either 10 ($P > 0{\cdot}05$) or 20 ($P > 0{\cdot}2$) weeks after infusion. The densities of airway wall mast cells in BM $\rightarrow W/W^v$ mice at 10 and 20

weeks after bone marrow infusion were four- and two-fold lower, respectively, than those of age-matched +/+ mice ($P < 0{\cdot}02$).

Lung parenchyma

There were no mast cells in the lung parenchyma of W/W^v mice at any time point (Fig. 2b). The density of lung parenchymal mast cells in 18-week-old +/+ mice was significantly greater than that of 8-week-old +/+ mice ($P < 0{\cdot}02$), and there was no significant difference between 18- and 28-week-old +/+ mice ($P > 0{\cdot}06$). However, mast cell densities were far lower in lung parenchyma than in extraparenchymal airway walls. In BM → W/W^v mice, mast cells appeared in the lung parenchyma 10 weeks after bone marrow infusion, and their density increased slightly, although significantly, by 20 weeks after bone marrow infusion ($P < 0{\cdot}003$); the difference between mast cell densities at 15 and 20 weeks after bone marrow infusion was not statistically significant ($P > 0{\cdot}05$). At 10 and 20 weeks after bone marrow infusion, the densities of mast cells in the lung parenchyma of BM → W/W^v mice were 18- and five- fold lower, respectively, than those of age matched +/+ mice ($P < 0{\cdot}009$).

Spleen

No mast cells were detected in the spleens of W/W^v mice at any time point examined (Fig. 3). There was no significant increase in splenic mast cell density in +/+ mice between 8 and 28 weeks of age. Mast cells appeared in the spleens of BM → W/W^v 5 weeks after infusion, and their density was significantly greater by 10 weeks ($P < 0{\cdot}03$). At 10 and 20 weeks after bone marrow infusion, splenic mast cell densities in BM → W/W^v mice were approx. five- and seven-fold greater than those of their age-matched +/+ mice.

Stomach mucosa

All stomach tissues of W/W^v mice were negative for mast cells at each time point examined (Fig. 4a). In the mucosa, the mast cell density of 18-week-old +/+ mice was slightly, albeit significantly ($P < 0{\cdot}05$), greater than that of 8-week-old +/+ mice. However, the mast cell density at 28 weeks was similar to that of 8-week-old +/+ mice ($P > 0{\cdot}07$). In BM → W/W^v mice, mast cells appeared in the mucosal area of the glandular stomach as early as 2·5 weeks after bone marrow infusion. The density of mast cells in the mucosa at 5 weeks after bone marrow infusion was significantly greater than at 2·5 weeks after bone marrow infusion ($P < 0{\cdot}0004$), but was lower than the maximal density that occurred 10 weeks after infusion. At 10 and 20 weeks after bone marrow infusion, mast cell densities were significantly greater than those of +/+ mice at the same age ($P < 0{\cdot}005$).

Stomach submucosa

There was no significant change in the density of mast cells in the stomach submucosa of +/+ mice from 8 to 28 weeks of age at each time point examined, and the mast cell densities were much greater (Fig. 4b) than those in the mucosa. Mast cell density in the submucosa of BM → W/W^v mice increased significantly between 2·5 and 5 ($P < 0{\cdot}0004$), 5 and 10 ($P < 0{\cdot}03$), and 10 and 15 ($P < 0{\cdot}02$) weeks after infusion, but not between 15 and 20 weeks ($P > 0{\cdot}3$). Mast cell densities in the submucosa of BM → W/W^v mice were approx two- and five-fold greater at 10 and 20 weeks after bone marrow infusion, respectively, than those of age-matched +/+ mice (Fig. 4b), and the differences at both time points were significant ($P < 0{\cdot}007$ and $P < 0{\cdot}0006$, respectively).

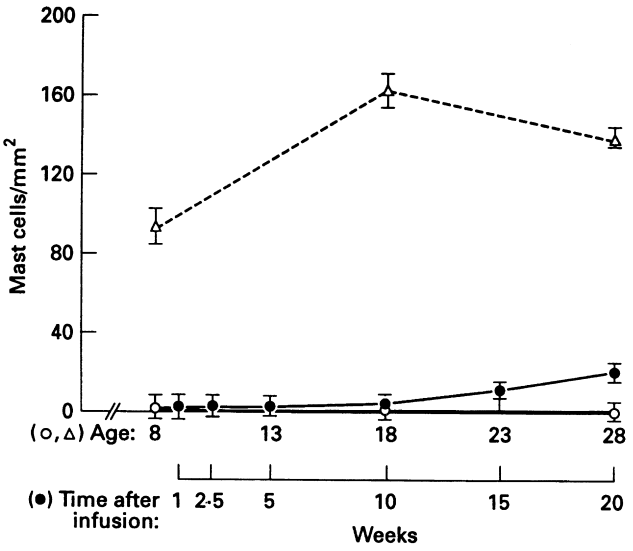

Fig. 1. Densities of mast cells in the skin of W/W^v (○), +/+ (△), and BM → W/W^v mice (●) mice. Date are expressed as mean ± s.e.m., $n = 6$.

Liver

Mast cells were not present in the liver of W/W^v mice. Mast cells were present in only one of each of six liver samples of 18-week-old +/+ mice (0·83 mast cells/mm^2) and 28-week-old +/+ mice (0·15 mast cells/mm^2). In BM → W/W^v mice, mast cells were seen in only four of six liver samples examined 15 weeks after infusion (0·04 ± 0·02 mast cells/mm^2 (mean ± s.e.m.)).

DISCUSSION

Our results indicate that the appearance of mast cells in several tissues of both +/+ mice and BM → W/W^v mice occurs asynchronously. Moreover, in BM → W/W^v mice, maximal mast cell densities are either abnormally higher or lower than those of age-matched +/+ mice, depending on the tissue. In the skin (Fig. 1), extraparenchymal airway walls (Fig. 2a), and lung parenchyma (Fig. 2b) of +/+ mice, mast cell densities did not reach maximal levels until 18 weeks of age. In contrast, in the spleen (Fig. 3), stomach mucosa (Fig. 4a), and stomach submucosa (Fig. 4b) of +/+ mice, mast cell densities had essentially reached maximal levels in animals 8 weeks of age, the earliest time point examined. The rank order of maximal mast cell densities reached in +/+ mice was as follows: skin ≈ extraparenchymal airway walls > stomach submucosa > stomach mucosa ≈ lung parenchyma > spleen. Thus, mast cell densities tended to be lower in those tissues where they reached a maximum earlier (Table 1).

In BM → W/W^v mice, maximal mast densities in the spleen, stomach mucosa, and stomach submucosa were five- to 13-fold higher than maximal mast cell densities in the corresponding tissues from +/+ mice. In contrast, maximal mast cell densities in the lung parenchyma, extraparenchymal airways, and skin were lower by two- to eight-fold in BM → W/W^v mice than in the corresponding tissues from +/+ mice (Table 1). Thus, in BM → W/W^v mice, there were abnormally high mast cell densities in those tissues that in +/+ mice reached maxima early (i.e. at 8 weeks of age), and there were abnormally low mast cell densities in those tissues that in +/+

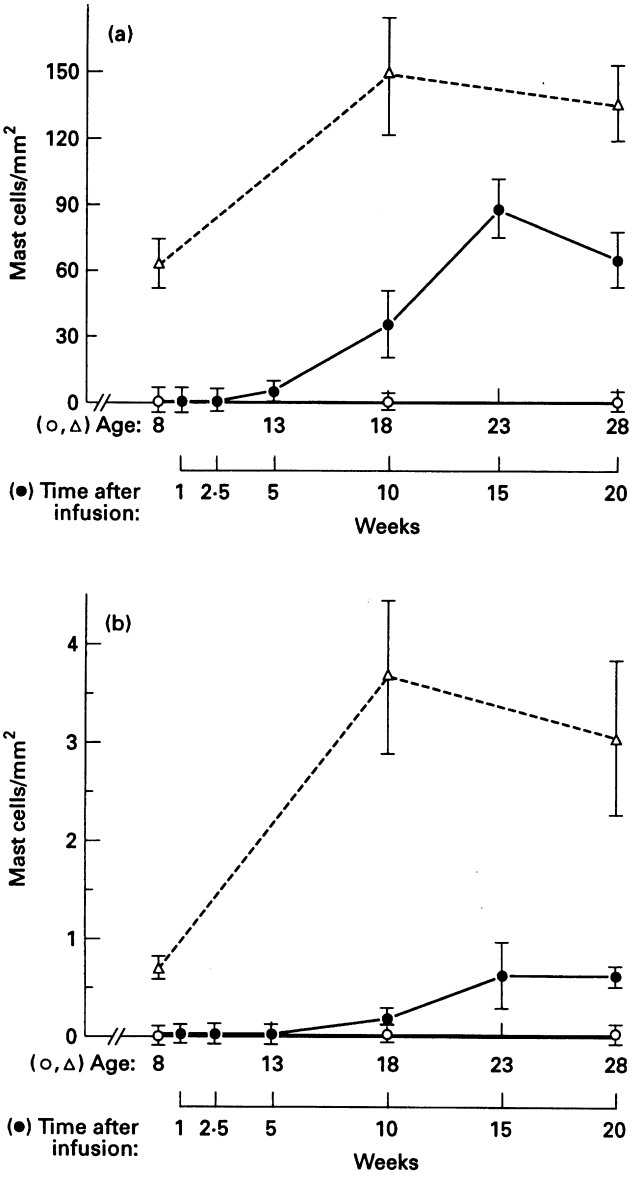

Fig. 2. Densities of mast cells in the walls of extraparenchymal airways including trachea and main bronchi (a) and in the lung parenchyma (b) of W/W^v (○), $+/+$ (△), and BM → W/W^v (●) mice. Data are expressed as mean ± s.e.m., $n = 6$.

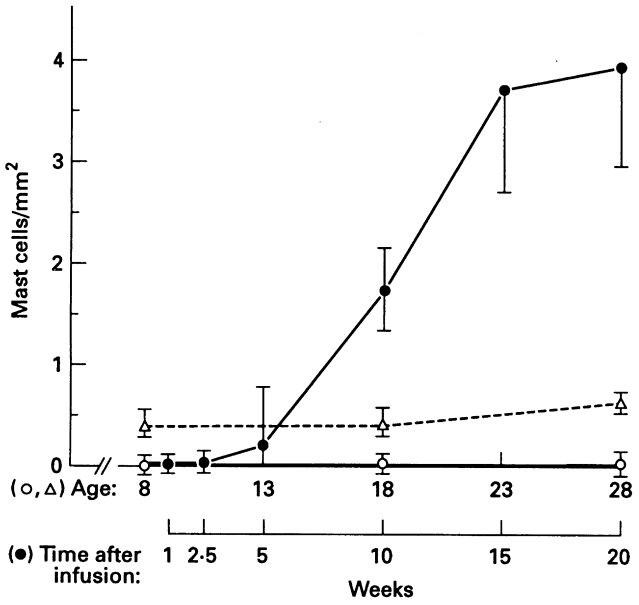

Fig. 3. Densities of mast cells in the spleen W/W^v (○), $+/+$ (△), and BM → W/W^v (●) mice. Data are expressed as mean ± s.e.m., $n = 6$.

mice reached maxima later (18 weeks of age). These findings indicate that there are differences in the homing and/or proliferation of blood-derived mast cell progenitors in the tissues studied, which may reflect tissue-specific expression of counterreceptors for adhesion molecules on the progenitors. In addition, the studies show that the introduction of a bolus of normal bone marrow progenitors in W/W^v mice results in mast cell densities in the studied tissues that do not mimic those of $+/+$ mice./ This finding suggests that the density of mast cell progenitors in the blood affects their development in tissues, perhaps as a result of cell–cell interactions that occur only when progenitors are present at high concentrations.

Three patterns were found in the time course of mast cell appearance in the tissues of BM → W/W^v mice. Stomach mucosa acquired mast cells the fastest, reaching maximal levels by 10 weeks after bone marrow infusion. Spleen, lung parenchyma, and extraparenchymal airway walls had an intermediate rate of mast cell appearance, with maxima at 15 weeks after infusion. Stomach submucosa and skin were the slowest to populate, and may not have reached maximal densities by 20 weeks after infusion, the last time point examined. There appeared to be no relationship between this order of appearance and either the respective maximal densities of mast cells reached in these tissues in BM → W/W^v mice, or the time course of mast cell appearance in these tissues in $+/+$ mice. Thus, the time course of mast cell appearance in these tissues in BM → W/W^v mice is not patterned after that of $+/+$ mice.

Previously, Kitamura *et al*. [4] reported the time course of mast cell appearance in the back skin and stomach of BM → W/W^v mice, as well as the mast cell density in several other sites at 15 weeks after bone marrow infusion. The data in that study were obtained from tissues fixed in 10% neutral buffered formalin, which is not suitable for the subsequent staining of mucosal mast cells with cationic dyes [1–3]. In addition, the data were derived by determining the ratio between mast cell numbers and tissue sample length, a semiquantitative method. In the present study, quantitative data have been obtained with morphometric area methods, and tissues were fixed in Carnoy's solution to account for all known classes of mast cells. Nonetheless, in the previous study a difference in the rates of mast cell appearance in back skin and stomach of $+/+$ mice was noted. In addition, the density of mast cells in the back skin of BM → W/W^v mice at 15 weeks after infusion was lower than that in $+/+$ mice. Similarly, Martin *et al*. [12] found that the density of mast cells in 2% paraformaldehyde/2·5% glutaraldehyde/0·025% $CaCl_2$-fixed sections of ear skin was lower in BM → W/W^v mice than in age-matched $+/+$ mice.

In contrast to skin, Kitamura *et al*. [4] found that the densities of mast cells in the forestomach and glandular stomach of BM → W/W^v mice were higher than in $+/+$ mice, and Galli *et al*. [13] found that the density of mast cells in the submucosa of the glandular stomach of BM → W/W^v mice 10 weeks after infusion was approx, two-fold higher than that of $+/+$ mice. These findings

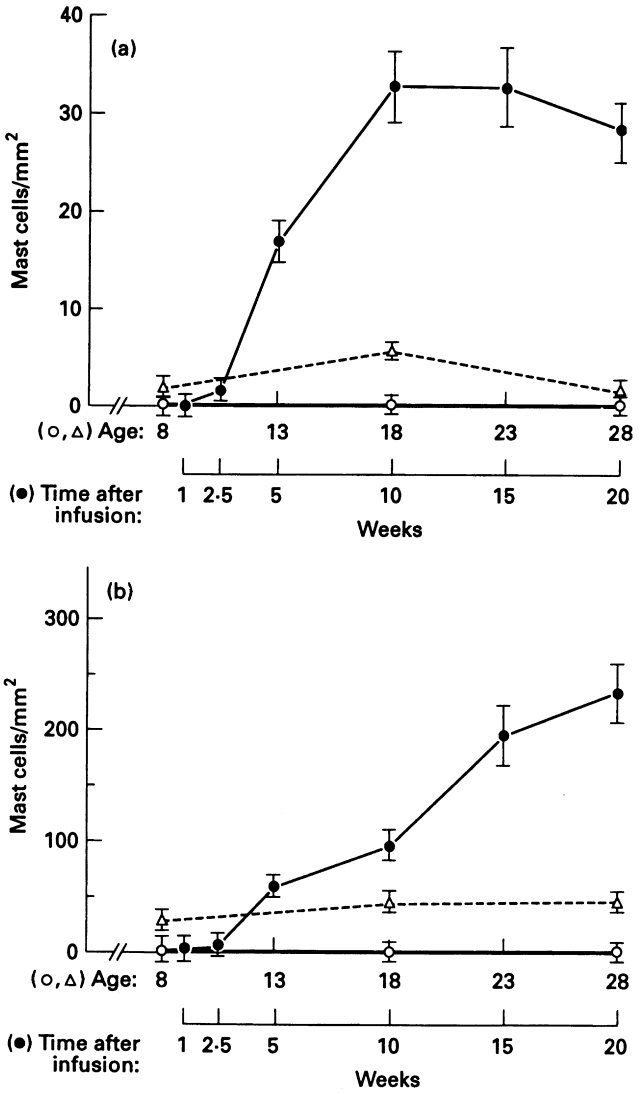

Fig. 4. Densities of mast cells in stomach mucosa (a) and stomach submucosa (b) of W/W^v (○), $+/+$ (△), and BM → W/W^v (●) mice. Data are expressed as mean ± s.e.m., $n = 6$.

are analogous to those presented here for stomach mucosa. In contrast, Galli *et al*. [13] also found that the density of mast cells in the mucosa of the glandular stomach of BM → W/W^v mice 10 weeks after infusion was normal. It is possible that the different results between the studies may relate to differences in the age of W/W^v mice at the time of bone marrow infusion. For example, Martin *et al*. [14] found no significant difference between the density of tracheal and peribronchial mast cells in $+/+$ mice and in BM → W/W^v mice 12–15 weeks after infusion at age 12–16 weeks. However, our studies reveal that it is critical to compare mast cell densities in age-matched $+/+$ and BM → W/W^v mice. As can be seen in Fig. 2a, the densities of mast cells in the extraparenchymal airway walls of 8-week-old $+/+$ mice and in BM → W/W^v mice 15 weeks after infusion are approximately equal, but the densities in the $+/+$ mice have not reached maximum at this time point; the same is true for mast cells in lung parenchyma (Fig. 2b). Thus, we found significantly lower densities of pulmonary mast cells in BM → W/W^v mice when the mice were infused

Table 1. Comparison of mast cell densities in $+/+$ and BM → W/W^v mice

Tissue	Maximal mast cell density (mast cells/mm²)	
	$+/+$ mice (age)*	BM → W/W^v mice (time)†
Skin	164 (18)	19 (20)
Extraparenchymal airway walls	149 (18)	89 (15)
Lung parenchyma	3·7 (18)	0·63 (15)
Spleen	0·41 (8)	3·6 (15)
Stomach mucosa	1·9 (8)	33 (10)
Stomach submucosa	30 (8)	235 (20)

* Age (weeks) of $+/+$ mice at which maximum density was reached.
† Time (weeks) after infusion at which maximum density was reached.

at 8 weeks of age and then matched for age in subsequent comparisons.

Our finding that the tissues of BM → W/W^v mice, including pulmonary sites, contain abnormal densities of mast cells has important implications for studies in which these mice are used to examine the role of mast cells in inflammatory processes. The data reveal that it is necessary to consider the possible contribution of abnormal mast cell density on the outcome of a response that is tested in BM → W/W^v mice, particularly if the inflammatory challenge is systemic. For example, our previous studies [15] showed that infusion of bonemarrow cells into W/W^v mice restored anti-IgE-induced pulmonary hyperresponsiveness to methacholine, despite the fact that the density of pulmonary mast cells was lower than that of $+/+$ mice. This distinction is even more notable in W/W^v mice that have been infused with IL-3 dependent bone-marrow-derived mast cells, where the density of tracheal mast cells is >15-fold lower than that in $+/+$ mice, suggesting minimal reconstitution, yet the infusion of anti-IgE into these mice elicits pulmonary hyperresponsiveness to methacholine that is comparable to that of $+/+$ mice [15]. The extensive degranulation of non-pulmonary mast cells stained for metachromasia with methylene blue has recently been recognized in these mice after the infusion of anti-IgE (T. Du, unpublished observation). Thus, the role of mediators derived from distal mast cells must be considered in systemic reactions when the tissue being assessed for the critical biologic response in BM → W/W^v mice contains far fewer mast cells than the same tissue in $+/+$ mice. On the other hand, in certain types of locally contained inflammation, such as passive cutaneous anaphylaxis [16] and dermal application of phorbol myristate acetate (PMA) [17] or substance P [18], local mast cells in BM → W/W^v mice may contribute substantially, even though their density is considerably lower than for normal $+/+$ mice.

In this study, quantitative morphometric determinations of the time courses of mast cell appearance in six tissues in age-matched $+/+$ and BM → W/W^v mice have revealed inter-tissue asynchrony in mast cell appearance *in situ* within each group of mice, as well as marked differences in tissue mast cell density between the two groups of mice. Indeed, the studies indicate that many tissues of BM → W/W^v mice are not 'reconstituted' with mast cells relative to the same tissues of age-matched $+/+$ mice, but rather exhibit markedly increased or decreased mast cell densities. Thus, in

addition to the recognition that abnormal mast cell localization and/or phenotype may occur in BM → W/W^v mice [19], the existence of abnormal mast cell density in multiple tissues must also be considered when comparing responses in W/W^v and BM → W/W^v mice.

ACKNOWLEDGMENTS

Supported by grants AI22531, AI32101, HL36110, and RR05950 from the National Institutes of Health, and a grant from the Natural Science and Engineering Research Council of Canada.

REFERENCES

1 Enerback L. Mast cells in rat gastrointestinal mucosa. I. Effects of fixation. Acta Pathol Microbiol Scand 1966; **66**:289–302.

2 Ruitenberg EJ, Elgersma A. Absence of intestinal mast cell response in congenitally athymic mice during *Trichinella spiralis* infection. Nature 1976; **264**:258–60.

3 Wingren U, Enerback L. Mucosal mast cells of the rat intestine: a re-evaluation of fixation and staining properties, with special reference to protein blocking and solubility of the granular glycosaminoglycan. Histochemical J 1983; **15**:571–82.

4 Kitamura Y, Go S, Hatanaka K. Decrease of mast cells in W/W^v mice and their increase by bone marrow transplantation. Blood 1978; **52**:447–52.

5 Geissler EN, Ryan MA, Housman DE. The dominant-white spotting (W) locus of the mouse encodes the c-kit proto-oncogene. Cell 1988; **55**:185–92.

6 Nakano T, Sonoda T, Hayashi C *et al*. Fate of bone marrow-derived cultured mast cells after intracutaneous, intraperitoneal, and intravenous transfer into genetically mast cell-deficient W/W^v mice. Evidence that cultured mast cells can give rise to both connective tissue type and mucosal mast cells. J Exp Med 1985; **162**:1025–43.

7 Otsu K, Nakano T, Kanakura Y *et al*. Phenotypic changes of bone marrow-derived mast cells after intraperitoneal transfer into W/W^v mice that are genetically deficient in mast cells. J Exp Med 1987; **165**:615–27.

8 Sonoda T, Ohno T, Kitamura Y. Concentration of mast-cell progenitors in bone marrow, spleen, and blood of mice determined by limiting dilution analysis. J Cell Physiol 1982; **112**:136–40.

9 Du T, Sapienza S, Eidelman DH, Wang NS, Martin JG. Morphometry of the airways during late responses to antigen challenge in the rat. Am Rev Respir Dis 1991; **143**:132–7.

10 Du T, Xu LJ, Lei M, Wang NS, Eidelman DH, Ghezzo H, Martin JG. Morphometric changes during the early airway response to allergen challenge in the rat. Am Dev Respir Dis 1992; **146**:1037–41.

11 James AL, Hogg JC, Dunn LA, Pare PD. The use of the internal perimeter to compare airway size and to calculate smooth muscle shortening. Am Rev Respir Dis 1988; **138**:136–9.

12 Martin TR, Ando A, Takeishi T, Katona IM, Drazen JM, Galli SJ. Mast cells contributes to the changes in heart rate, but not hypotension or death, associated with active anaphylaxis in mice. J Immunol 1993; **151**:367–76.

13 Galli SJ, Wershil BK, Bose R, Walker PA, Szabo S. Ethanol-induced acute gastric injury in mast cell-deficient and congenic normal mice. Evidence that mast cells can augment the area of damage. Am J Pathol 1987; **128**:131–40.

14 Martin TR, Galli SJ, Katona IM, Drazen JM. Role of mast cells in anaphylaxis. Evidence for the importance of mast cells in the cardiopulmonary alterations and death induced by anti-IgE in mice. J Clin Invest 1989; **83**:1375–83.

15 Martin TR, Takeishi T, Katz HR, Austen KF, Drazen JM, Galli SJ. Mast cell activation enhances airway responsiveness to methacholine in the mouse. J Clin Invest 1993; **91**:1176–82.

16 Wershil BK, Mekori YA, Murakami T, Galli SJ. ^{125}I-fibrin deposition in IgE-dependent immediate hypersensitivity reactions in mouse skin. Demonstration of the role of mast cells using genetically mast cell-deficiency mice locally reconstituted with cultured mast cells. J Immunol 1987; **139**:2605–14.

17 Wershil BK, Murakami T, Galli SJ. Mast cell-dependent amplification of an immunologically nonspecific inflammatory response. Mast cells are required for the full expression of cutaneous acute inflammation induced by phorbol 12-myristate 13-acetate. J Immunol 1988; **140**:2356–60.

18 Yano H, Wershil BK, Arizono N, Galli SJ. Substance P-induced augmentation of cutaneous vascular permeability and granulocyte infiltration in mice is mast cell dependent. J Clin Invest 1989; **84**:1276–86.

19 Galli SJ. New approaches for the analysis of mast cell maturation, heterogeneity, and function. Federation Proceedings 1987; **46**:1906–14.